MILLIMAN WHITE PAPER

Modelling the impact of climate risks on mortality

Detailed case studies on exposure to high temperatures, alternative modelling for vector-borne diseases

Alexandre Boumezoued
Amal Elfassihi
Valentin Germain
Eve-Elisabeth Titon

Milliman

Climate change, partly caused by human activities, is already having an impact on our society. According to the latest Intergovernmental Panel on Climate Change (IPCC) report of August 2021,[1] the concentration of CO_2 in the atmosphere was at its highest level in 2019 in the last 2,000 years.

An increase in Earth's surface temperature will cause several problems such as extreme changes in weather events (heat waves, heavy precipitation, droughts etc.) by increasing their frequency and intensity.

Two main impacts can be identified:

- The French Insurance Federation (FFA) has published a report[2] in which the impacts of climate change on the insurance sector in France are studied for 2040. The increase in the cost of claims due to climate change is estimated at 21 billion euros over the period 2014 to 2039 compared to 8 billion euros over the period 1988 to 2013. The study predicts that claims caused by natural hazards will reach 92 billion euros in 2040 (an increase of 90%).
- Climate change will also have an impact on health and mortality. According to a report[3] published by the World Health Organisation (WHO), between 2030 and 2050 climate change is expected to result in nearly 250,000 additional deaths per year globally due to childhood undernutrition, malaria, diarrhea and heat stress.

As these events will affect the whole world, (re)insurers will need to improve their models to cope with climate change: by having a better understanding of the climate phenomena and their consequences and by taking into account projection assumptions.

Executive Summary

For the main climatic causes of death, i.e., those for which there are a significant number of deaths, a Lee-Carter type of modelling can be applied.

The objective of this paper is to propose a model to capture the impact of climate risks on mortality. The model constructed is derived from a Lee-Carter model and is adapted to capture the impact of a specific cause on overall mortality rates. The risk considered in the following case studies is the "exposure to high temperatures" in France and in the US (at the state level: in this paper we will present the results obtained for the state of Oklahoma). The objective is to develop a model and make projections for mortality shock values.

The selected climate models for the different geographical areas studied include climate variables related to temperature. These variables explain the observed peaks in deaths due to summer heat waves. The global model includes a term capturing the global mortality without climatic causes, and a term modelling only the mortality due to high temperatures.

[1] IPCC. Climate Change 2021: The Physical Science Basis. Retrieved 7 December 2022 from https://www.ipcc.ch/report/ar6/wg1/.

[2] See https://www.mrn.asso.fr/wp-content/uploads/2018/05/etude_changement_climatique_et_assurance_a_lhorizon_2040.pdf

[3] WHO (5 December 2018). Health and Climate Change. Retrieved 7 December 2022 from https://www.who.int/news-room/facts-in-pictures/detail/health-and-climate-change.

The resulting model performs well in predicting observed mortality rates. Moreover, it performs better than a classic Lee-Carter model according to the R^2 and the Akaike information criterion (AIC) and Bayesian information criterion (BIC).

The impact of high temperatures is clearly observable at high ages (over 65 years). The mortality shocks—calculated according to the European Insurance and Occupational Pensions Authority (EIOPA) methodology—incorporating the modelling of the impact of high temperatures are on average 6.12% larger than the conventional shocks provided by a classic Lee-Carter model.

For climatic causes with fewer deaths, such as vector-borne diseases, it is not possible to apply the model developed earlier. Specific modelling needs to be explored: for mosquito-borne diseases, a refined Susceptible/Infected/Recovered (SIR)-type model could be appropriated.

Scope and data

SCOPE

For this paper, we chose to focus on France and a specific state in the US with one specific climatic cause: exposure to high temperatures.

In France, there have been significant heat waves: since 1947, 41 heat waves hit France with different intensities, with a major heat wave in 2003 (more than 12,000 deaths).

The climate in the US is not homogeneous throughout the country as not all states are subject to heat waves. The area extending over several states in the southwest of the US is the one presenting heat waves. As our model does not produce consistent results for states outside of this region, the state of Oklahoma, which is prone to heat waves, is selected to present the results.

DATA

This study combines the use of three databases: one for the mortality linked to the specific cause (Global Health Data), one for the global national mortality (Human Mortality Database) and one for the climate variables.

- **Global Health Data (GHD):** This database is published by the Institute for Health Metrics and Evaluation (IHME). GHD is constructed with the death numbers classified by different parameters (age, territory, years etc.) and particularly by the cause of death. The selection of death numbers relative to one specific risk or cause is possible on this database. On the “pollution” cause, for instance, we can find all the deaths caused by pollution, including deaths occurring from the increase in prevalence of type 2 diabetes due to exposure to pollution. This database considers mortality estimates found in the literature and has a history from 1990 to 2019.

FIGURE 1: FRENCH DEATH RATE ATTRIBUTABLE TO HIGH TEMPERATURE EXPOSURE (BOTH SEXES, FRANCE, FOR 100,000)

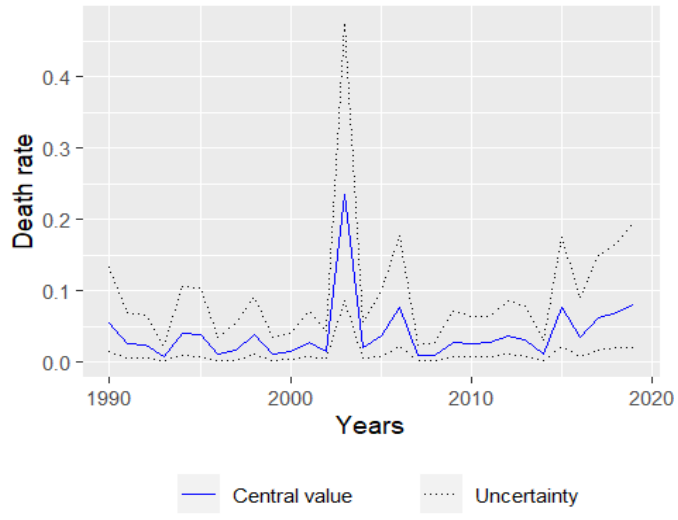

Source: GBD database.

- **Human Mortality Database (HMD):** The HMD is the reference for the death data used for actuarial purposes [3]. The calibration period is from 1990 to 2018.
- **Climatic and meteorological database:** This database contains several climate variables including the temperature, rainfall, sunny period and wind-related data whose source depends on the country considered.

  The database containing the climatic variables for France is provided by Météo France.[4] The climate variables include the number of days above a certain temperature (30°C, 35°C, 40°C), rainfall, wind-related data, sunny period and minimum/maximum/mean temperatures. All the data are classified by monthly values and by stations located through France. The history is from 1990 to 2021. Moreover, a relevant period to focus on the high temperatures is defined: the variables are built on summertime (June, July and August), in order to better capture the effect of heat waves.

  The US study is based on climate variables from the Global Historical Climatology Network Daily (GHCND) database provided by the National Oceanic and Atmospheric Administration (NOAA). The database contains daily weather information for over 10,000 stations in the US. Per weather station and per day, several climate variables are available such as recorded temperatures. For each weather station and for each day since 1990, the maximum and minimum recorded temperatures are kept in order to construct variables such as the maximum temperature per month, or the number of days exceeding different high temperature thresholds.

Modelling

ADAPTATION OF THE CLASSICAL LEE-CARTER MODEL

The first goal of the study is to implement a model which captures the mortality due to climatic causes. The proposed model derives from a Lee-Carter model [2], which has been adapted to isolate the mortality due to the climate.

$$\ln(\mu_{x,t}) = \alpha_x + \beta_x^o \kappa_t^o + \delta_x^c C_t$$

The purpose of the term $\boldsymbol{\beta_x^o \kappa_t^o}$ is to capture the global mortality which does not consider the climate cause. Note that $\boldsymbol{c}$ is related to the climate cause of mortality while $\boldsymbol{o}$ is related to other causes.

The main objective of this model is to capture the difference of mortality on a specific climatic cause. The final goal is to compute mortality shocks and compare them to the shocks computed by a classic Lee-Carter model.

CONSTRUCTION OF A CLIMATE INDEX

Considering all the available climate variables, the goal is to select the best climate variables that can explain the mortality rates related to the climate cause. The method used is a linear regression. To select the best variables, a `stepAIC` procedure is performed: this method computes the AIC by calculating all the possible variable combinations that provide a minimal AIC. This method is applied on the climate variables.

Then a p-value study is performed to find what are the best climate variables to explain the global mortality rates of the climate cause. The more significant climate variables are chosen.

Thus, the final climate index $\boldsymbol{C_t}$ follows the following three-parameter linear equation:

$$C_t = a + b^T X_t$$

where $\boldsymbol{a, b}$ are the linear regression parameters, and $\boldsymbol{X_t}$ is the vector of climate variables of year $\boldsymbol{t}$.

HARVESTING EFFECT

The harvesting effect refers to the fact that fragile people are primarily affected by an event that causes excess mortality in the general population. Without this event, these people would have died in the days or weeks that follow. The consequence of this harvesting effect is that the event is followed by a period of under-mortality.

[4] Météo France. Public Data. Retrieved 7 December 2022 from https://donneespubliques.meteofrance.fr/?fond=produit&id_produit=115&id_rubrique=38.

To model this effect, two parameters are added to the climate index combining the climate data of the year of study and the previous year.

$$CI_t = a + \alpha(b^T X_t) + \gamma(b^T X_{t-1})$$

where $\boldsymbol{\alpha}$ represents the immediate climate impact, and $\boldsymbol{\gamma}$ represents the harvesting effect.

AGE RANGE CONSTITUTION

Climate mortality impacts the population differently by age. For this reason, a division of ages into three classes is considered in order to reflect the impact of climate mortality by age while remaining at a sufficiently large scale to have enough deaths in each age class. Moreover, this division depends on data availability.

For the following, we set:

- $x_0 = 0, x_1, x_2, x_3 = 111$
- The age classes are built as: $\forall i \in [0,2], c_i = [x_i, x_{i+1} - 1]$

MODEL

The calibration of the model is done in three steps. The final calibration step considers continuous ages, whereas the first steps of the calibration consider age classes in order to more accurately calibrate the mortality related to climate risk. The beginning equation for the calibration process is the following:

$$\ln(\mu_{c_i,t}) = \alpha_{c_i} + \beta_{c_i}\kappa_t + \delta_{c_i}C_t$$

1. **Estimation of mortality related to climate risk:**

$$\ln(\mu_{c_i,t}) = \alpha_{c_i} + \beta_{c_i}\kappa_t + \boldsymbol{\delta_{c_i}C_t}$$

   a. **Calibration of $\boldsymbol{\alpha_{c_i}}$** by using a Lee-Carter model on 1990-2018 mortality data (HMD). The α_{c_i} is three vector parameters for the three age classes.

   b. **Calibration of the climate index ($\boldsymbol{a, b}$)** by using a linear regression between the death rate of the climate cause and climate variables (see the *Construction of a Climate Index section above*).

   c. **Calibration of $\boldsymbol{\delta_{c_i}}$**, by minimising the residuals without the harvesting effect, which are

$$R_{c_i,t} = \ln(\mu_{c_i,t}) - \alpha_{c_i} - \delta_{c_i}C_t$$

   During this calibration, a peak function is used to emphasise the mortality excess of each age class.

2. **Integration of the harvesting effect:** By the calibration of α, β. This step integrates the harvesting effect by replacing C_t by CI_t. The harvesting parameters are found by minimising the previous residuals with the harvesting effect:

$$R_{c_i,t} = \ln(\mu_{c_i,t}) - \alpha_{c_i} - \delta_{c_i}(a + \alpha(b^T X_t) + \gamma(b^T X_{t-1}))$$

3. **Calibration of the global age-continuous mortality rates**: At this final step, we convert all the age-class parameters in age parameters, and the equation becomes:

$$\ln(\mu_{x,t}) = \boldsymbol{\alpha_x} + \boldsymbol{\beta_x\kappa_t} + \delta_x CI_t$$

   We consider for this part the following residuals (by removing the α_x):

$$R_{x,t} = \ln(\mu_{x,t}) - \delta_x CI_t$$

   Final calibration consists in applying a Lee-Carter model on the residuals $R_{x,t}$ to find the $\boldsymbol{\alpha_x, \beta_x}$ and $\boldsymbol{\kappa_t}$ parameters.

France case study: Heat exposure

The age groups chosen for France are, according to the available data, 0-25 years (young people), 25-65 years (working population), and 65 years and over (seniors).

The variables selected for the construction of the climate index are:

- T_t^{35}: The average number of days where the temperature is above 35°C during summertime of year t.
- T_t^{40}: The average number of days where the temperature is above 40°C during summertime of year t.

The two climate variables (Figure 2) are correlated with a 62.54% coefficient, but they are kept because they do not have the same level of information and are useful to explain the death rates.

FIGURE 2: AVERAGE NUMBER OF DAYS ABOVE 35°C (LEFT) AND 40°C (RIGHT) DURING SUMMERTIME

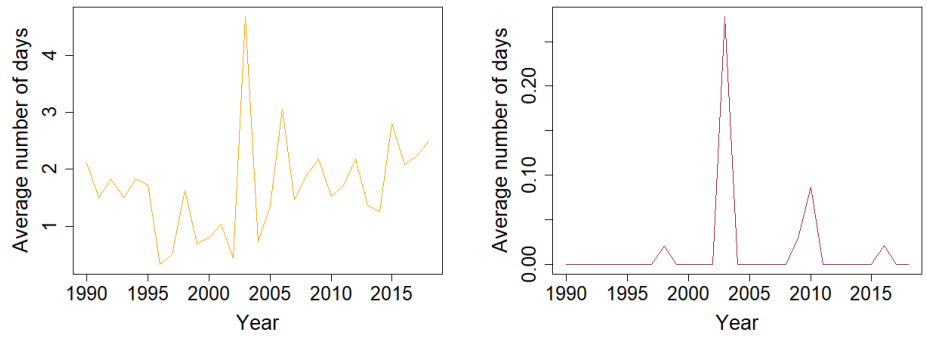

The climate index is constructed using the regression between the two climate variables and the climate mortality rates (Figure 3).

FIGURE 3: CLIMATE INDEX AND ORIGINAL DEATH RATE IN FRANCE

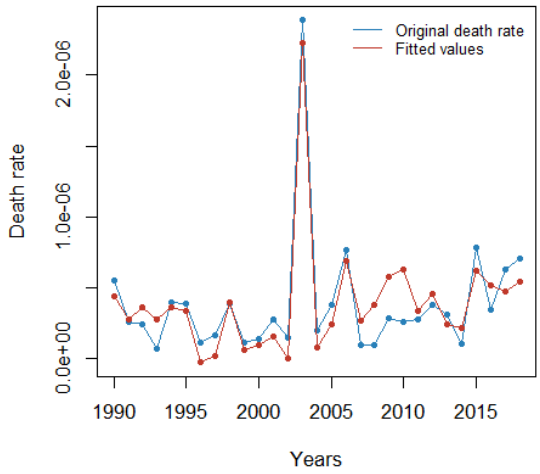

The fit is good ($\boldsymbol{R^2 \approx 86\%}$) and the trend of climate-caused mortality over time can be explained with only these two climate variables. Thus, the final climate index $\boldsymbol{C_t}$ follows a three-parameter linear equation:

$$C_t = a + bT_t^{35} + cT_t^{40}$$

where a, b, c are the linear regression parameters.

Figure 4 illustrates the three death rates: the original death rate (in blue), the death rate from a Lee-Carter model (in green) and the death rate for the climate Lee-Carter model (in red). Note that, for the age of 75, the two Lee-Carter models are very correlated.

FIGURE 4: COMPARISON OF THE DIFFERENT MODELLING – 75 YEARS OLD

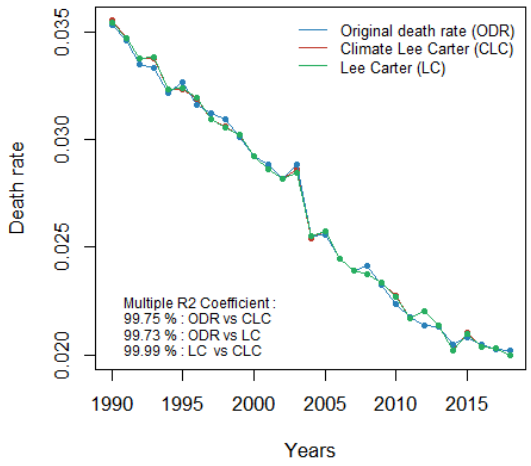

The R^2 coefficients between the original death rates and the Lee-Carter models are plotted in Figure 5. The two models are similar in the fit, but one can see that, on high ages, the climate model is better than the original Lee-Carter model.

The fit is computed between the two Lee-Carter models (classic and climate) and the original death rates, using the R^2 measure. The climate model is better than the Lee-Carter model on 61.82% of the ages (and on 93.64% of the ages if we consider a tolerance on the R^2 of 0.5%).

FIGURE 5: R^2 FITTING COEFFICIENTS BETWEEN THE TWO MODELS

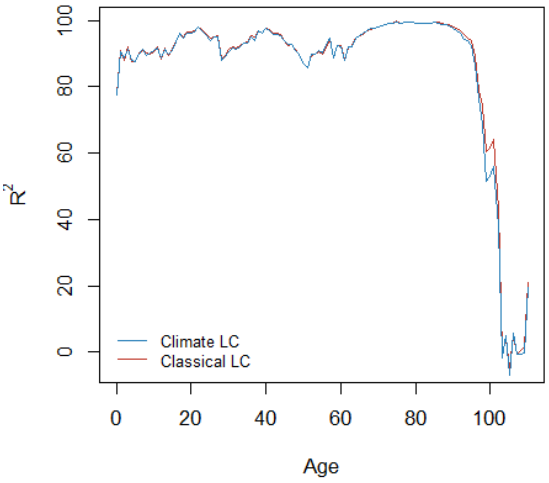

When evaluating the goodness-of-fit of different models, it is generally anticipated that models with more parameters provide a better fit to the data. To rule out the possibility that the better fit observed in a model is the result of over-parametrisation and to compare the relative performance of several models, we also use information criteria which modify the maximum likelihood criterion by penalising models with more parameters. Two of these criteria are the AIC and the BIC, with lower values of AIC and BIC being preferable. It can be observed that the climate Lee-Carter model has a lower AIC/BIC than its classic version, as shown by the table in Figure 6.

FIGURE 6: AIC/BIC BETWEEN THE TWO MODELS

CRITERION	CLASSIC LC	CLIMATE LC
AIC	42,877	42,453
BIC	44,390	43,966

US case study: Heat exposure in Oklahoma

Note that the age groups chosen for the US are slightly different from those used for France: 0-49 years, 50-69 years, and 70 years and over.

For the US, the climate index is built for each state. Therefore, the R^2 score of the regression of climatic mortality rates against climatic variables is variable across states (Figure 7). A selection of variables at the state level is made in order to build the climate index. The results vary from one state to another: for states that are minimally affected by heat waves, even if the R^2 score is correct, the model does not present consistent results.

FIGURE 7: R^2 SCORE BY STATE

The fit of climate mortality rates as a function of climate variables in Oklahoma is good ($\boldsymbol{R^2 \approx 92\%}$) and the trend of climate mortality over time can be explained with eight climate variables selected from 41 (Figure 8).

FIGURE 8: CLIMATE INDEX AND ORIGINAL DEATH RATE IN OKLAHOMA

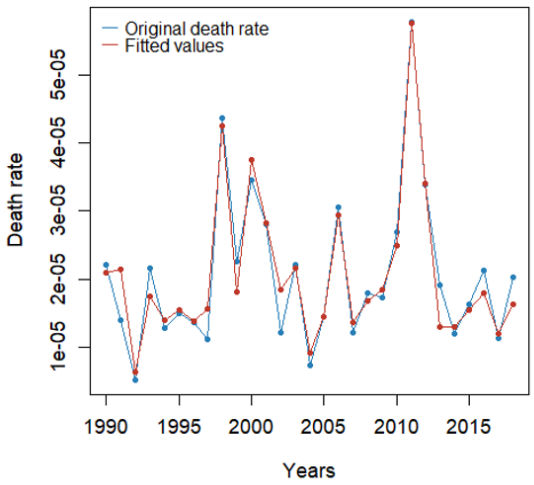

FIGURE 9: COMPARISON BETWEEN THE 3 OKLAHOMA DEATH RATES FOR 75 YEARS OLD

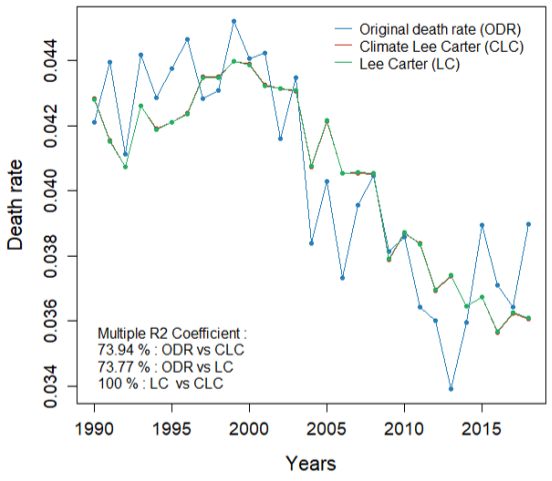

Figure 9 provides a comparison of the original death rates, classic Lee-Carter model results and climate Lee-Carter model results in Oklahoma. For the age of 75, the two Lee-Carter models are very correlated, the climate Lee-Carter is slightly better than the classic Lee-Carter model (73.94% against 73.77%).

FIGURE 10: R^2 FITTING COEFFICIENTS BETWEEN THE TWO MODELS

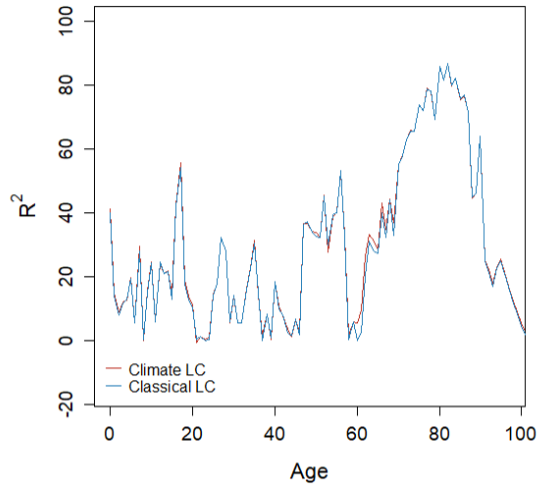

The R^2 coefficients between the original death rates and the Lee-Carter models are plotted in Figure 10. The two models are similar in the fit, but one can see that, on high ages, the climate model is better than the original Lee-Carter model. However, contrary to France, the R^2 coefficient of both the climate Lee-Carter model and the classic model is much lower, especially for young ages.

As for the French case study, it can be observed that the climate Lee-Carter model has a lower AIC/BIC than its classic version, as shown by the table in Figure 11.

FIGURE 11: AIC/BIC BETWEEN THE TWO MODELS

CRITERION	CLASSIC LC	CLIMATE LC
AIC	34,792	34,715
BIC	36,306	36,229

Projections – results for French case study

The classic method to project a Lee-Carter model is to use an autoregressive process. The temporal parameter κ_t is simulated according to the following equation:

$$\kappa_t = \kappa_{t-1} + \theta + \varepsilon_t$$

where $\varepsilon_t \sim \mathcal{N}(0, \sigma^2)$.

To calculate the mortality shocks for the climate model, an autoregressive model is applied. The projection method must consider both time parameter κ_t and the climate variables matrix X_t . This method allows us to jointly project the three-time series according to the correlations between them:

$$(X_t, \kappa_t) = (X_{t-1}, \kappa_{t-1}) + (\mu_1, \mu_2) + C(\epsilon_t^1, \epsilon_t^2)$$

The vector (μ_1, μ_2) is the mean vector of the time series (X_t, κ_t), and C is the Cholesky decomposition of the variance-covariance matrix Σ where $\Sigma = CC'$. This method is used for the first year only and prolonged by mean to the following years (the noise is set to 0).

We performed 2,500 simulations for ages from 40 to 90 years old, according to the previous method with a one-year time horizon.

The one-year projections of the two models for death rates in France (Figure 12) are very similar due to the high correlation rate of the model calibration. The differences are visible at 65 years old and higher: the plot of the impact of the climate cause shows this fact more obviously (Figure 13). Before 65 years old, the cause impact is negligible. For the ages above 65 years old the effect of high temperatures is preponderant and increases with age.

FIGURE 12: ONE-YEAR PROJECTION – FRANCE

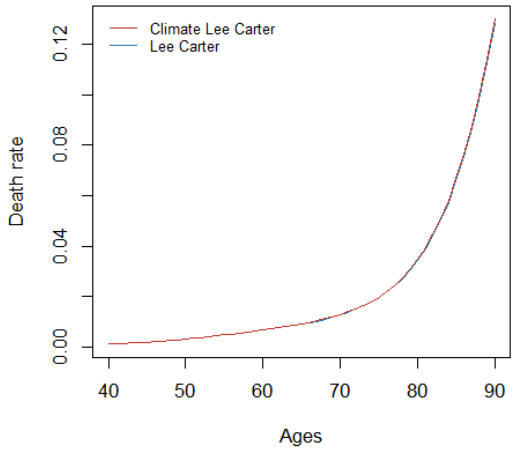

FIGURE 13: IMPACT OF CLIMATIC CAUSE – FRANCE

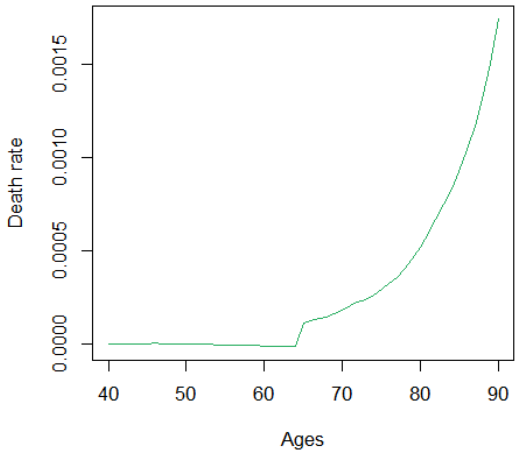

Shock calculation

METHODOLOGY

Step 1: The calibration method used to compute shock values is the one presented by EIOPA. It combines three steps, recalled in [4]. Simulations of 2,500 future mortality tables are performed at a one-year horizon (projection part).

Step 2: Life expectancies are calculated for each attained age given the survival function determined by the simulated mortality tables. The 0.5th percentile realisations of the cohort life expectancies are then computed.

Because mortality sensitivity can be captured by changes in life expectancies, such optimal stresses can be determined by analysing their impact on life expectancies. For each age, the optimal mortality shock is defined as the stress which matches the shocked central life expectancy with the 0.5th percentile of the not shocked life expectancy.

The age-dependent shocked life expectancy is defined according to:

$$e_x^h(t) = \frac{1}{2} + \sum_{k=1}^{+\infty} \prod_{s=0}^{k-1} \left(1 - (1+h) q_{x+s}(t+s)\right)$$

Step 3: For each age, the optimal mortality shocks are defined as the shocks that minimise the distance between the life expectancy in the central scenario and the quantile realisation.

$$h_{\inf}(x) = \underset{h \in]-1,1[}{\operatorname{argmin}} \left(e_x^h(t) - e_x^{0.5\%}(t) \right)^2$$

Through this process, mortality shocks are obtained for each age.

RESULTS FOR FRANCE

As expected, the mortality shock values (Figure 14) obtained with the model that takes into account the climate risk are greater than the classic shocks, and a peak between 60 and 70 years old can be observed.

On the whole interval, the climate shocks are 6.12% greater on average than the classic shocks. On the 40 to 65 years old interval, the average classic shocks are 4.62% against 9.32% for the climate shocks. The average difference on the 65 to 90 years old interval is 7.61% for the climate shocks.

FIGURE 14: MORTALITY SHOCK VALUES

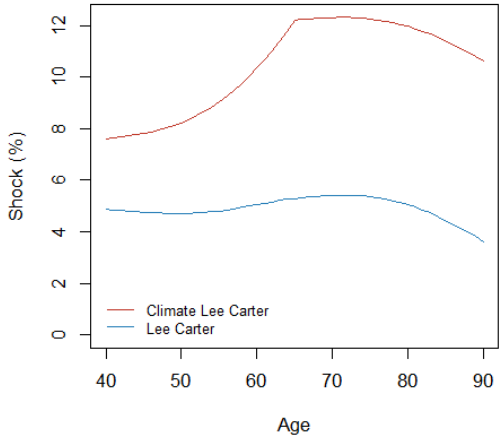

Case of vector-borne diseases

WHAT ARE THEY?

Vector-borne diseases are illnesses that are transmitted by arthropod vectors, which include mosquitoes, ticks and fleas. These vectors can carry infective pathogens such as viruses, bacteria and protozoa, which can be transferred from one host to another.

Vector-borne diseases account for more than 17% of all infectious diseases worldwide, causing more than 700,000 deaths annually, with more than 50% of the world's population currently estimated at risk of infection with a vector-borne pathogen [5].

Mosquito-borne diseases are a key group of concern as they include both very high burden and important emerging diseases, including human malaria (around 212 million cases per year), dengue (around 96 million cases per year), chikungunya (around 693,000 cases per year) and Zika virus disease (around 500,000 cases per year).[5]

A MODELLING APPROACH EXAMPLE

Causes of death with too few deaths, such as vector-borne diseases, cannot be modelled by a Lee-Carter model: alternative models more adapted to the specificities of the cause of death must be developed.

Following [6], mosquito-borne diseases can be modelled by a refined SIR-type model. Unlike classic SIR-type models, two populations have to be modelled: human individuals and mosquito vectors.

- **Human individuals:** They start in a susceptible state S_h and then can be infected through bites of infectious mosquito vectors I_m at rate a and with the probability b. When infected, these individuals change to the exposed state E_h. They become infectious and symptomatic (I_h^1) with the probability $\omega_h(1 - p_a)$, or asymptomatic (I_h^2) with the probability $\omega_h p_a$. Finally, infectious individuals become recovered R at rate σ and cannot be infected again.

[5] Data are from WHO.

- **Mosquitoes:** If a susceptible mosquito vector S_m bites an infectious human at rate a, the mosquito can become exposed (E_m) with the probability c and then infectious (I_m) at the rate ω_m, characterised by the inverse of the extrinsic incubation period. Note that the infection probability of a susceptible mosquito exposed to the pathogen c is dependent on both the local temperature and the degree of adaptation of the mosquito to its environment.

FIGURE 15: COMPONENT DIAGRAM FOR A VECTOR-BORNE DISEASE SIR-TYPE MODEL

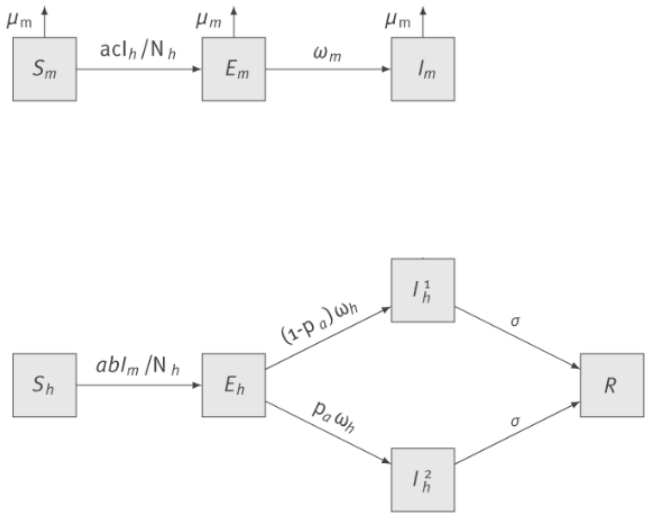

VECTOR-BORNE DISEASES AND CLIMATE CHANGE

There are many signals that climate change has already affected vector-borne disease transmission or spread. For example, a time-series analysis of monthly malaria cases in the highlands of Colombia and Ethiopia provided evidence for a shift in the altitudinal distribution of malaria towards higher altitudes in warmer years, suggesting that, in the absence of intervention, the malaria burden will increase at higher elevations as the climate warms [7].

Besides, in the US, higher cumulative growing degree days, lower cumulative precipitation and lower saturation deficit (inversely related to humidity) were found to be associated with an earlier start to the Lyme disease season [8].

Climate change is likely to have both short-term and long-term effects on vector-borne disease transmission and infection patterns. However, following [9], predicting how future climate change will affect vector-borne diseases seems very challenging due to numerous uncertainties, including:

- Future climate change will depend on human actions to reduce greenhouse gas emissions
- Prediction would need to take into account changes in non-climate drivers such as social and environmental ones, many of which are also unpredictable

In order to make projections, models can be based on alternative scenarios to have an understanding of a range of possible futures. Projections about the future incidence and distribution of specific vector-borne diseases can be made by associating a future climate change scenario with a vector-borne disease model that has been validated using historical data. The approach can also incorporate scenarios for non-climate drivers such as travel, socioeconomic factors or public health advances.

According to [10], although the effects of climate change on mosquito-borne disease risk are significant, the influence of other global change processes and their interactions occur over shorter timescales and are likely to have a greater impact in the immediate future. Considering the effect of climate change in isolation might result in inaccurate predictions of mosquito-borne diseases risk. This issue is compounded by the fact that many studies do not account for the multiple sources of uncertainty in their predictions, including the data (e.g., health, environmental, socioeconomic), future global change scenarios (e.g., climate emission scenarios) and the structure of the models.

REFERENCES

[1] Milliman White Paper (May 2020). Living forever with Solvency II: A closer look at mortality stresses.

[2] Lee, R. D., & Carter, L. R. (1992). Modeling and forecasting.

[3] Human Mortality Database. The University of California, Berkeley (USA), and Max Planck Institute for Demographic Research (Germany). Available at www.mortality.org or www.humanmortality.de

[4] EIOPA (February 2018). EIOPA's second set of advice to the European Commission on specific items in the Solvency II Delegated Regulation.

[5] World Health Organisation (2014). A global brief on vector-borne diseases. No. WHO/DCO/WHD/2014.1.

[6] Sochacki, Thomas, et al. (2016). Imported chikungunya cases in an area newly colonised by Aedes albopictus: Mathematical assessment of the best public health strategy. Eurosurveillance 21.18: 30221.

[7] Siraj, A. S., Santos-Vega, M., Bouma, M. J., Yadeta, D., Carrascal, D. R., & Pascual, M. (2014). Altitudinal changes in malaria incidence in highlands of Ethiopia and Colombia. Science, 343(6175), 1154-1158.

[8] Moore, S. M., Eisen, R. J., Monaghan, A., & Mead, P. (2014). Meteorological influences on the seasonality of Lyme disease in the United States. The American journal of tropical medicine and hygiene, 90(3), 486.

[9] Rocklöv, Joacim, and Robert Dubrow (2020). Climate change: An enduring challenge for vector-borne disease prevention and control. Nature immunology 21.5: 479-483.

[10] Franklinos, Lydia HV, et al. (2019). The effect of global change on mosquito-borne disease. The Lancet Infectious Diseases 19.9: e302-e312.

Milliman

Milliman is among the world's largest providers of actuarial, risk management, and technology solutions. Our consulting and advanced analytics capabilities encompass healthcare, property & casualty insurance, life insurance and financial services, and employee benefits. Founded in 1947, Milliman is an independent firm with offices in major cities around the globe.

milliman.com

CONTACT

Alexandre Boumezoued
Alexandre.boumezoued@milliman.com

Amal Elfassihi
Amal.Elfassihi@milliman.com

Valentin Germain
Valentin.Germain@milliman.com

Eve-Elisabeth Titon
EveElisabeth.Titon@milliman.com